

1        **Land Productivity Dynamics Indicator: LPDynR**

2        **Package**

3            Xavier Rotllan-Puig<sup>1,2,<sup>✉</sup></sup>, Eva Ivits<sup>3</sup> and Michael Cherlet<sup>1</sup>

4            **Version under development (14/12/2020)**

5       <sup>1</sup> Joint Research Centre – European Commission. Directorate D – Sustainable Resources.

6        Unit D6 – Knowledge for Sustainable Development & Food Security Unit. Via Enrico  
7        Fermi 2749. I-21027 Ispra (VA), ITALY

8       <sup>2</sup> ASTER-Projects. Barri Reboll, 9, 1r. 08694 Guardiola de Berguedà (Barcelona), SPAIN

9       <sup>3</sup> Geospatial Information Services group, European Environment Agency, Copenhagen,  
10      DENMARK

11      <sup>✉</sup> Correspondence: Xavier Rotllan-Puig <xavier.rotllan.puig@aster-projects.cat>

12      **Abstract**

13      As part of the UN Sustainable Development Goal 15 (Life on Land), the indicator 15.3.1  
14      is adopted to measure the Land Degradation Neutrality (stable —or increasing— state  
15      regarding the amount and quality of land resources required to support ecosystem  
16      functions and services and enhance food security during a certain period of time). It is a  
17      binary indicator (i.e. degraded/not degraded), expressed as the proportion of land that is  
18      degraded over total land area, and is based on three sub-indicators: (1) Trends in Land  
19      Cover, (2) Land Productivity and (3) Carbon Stocks.

20 The Land Productivity sub-indicator (LP) refers to the total above-ground Net Primary  
21 Production and reflects changes in health and productive capacity of the land. Its  
22 declining trends can be usually understood as land degradation. LP is calculated using the  
23 Land Productivity Dynamics (LPD) approach, first developed by Ivits and Cherlet  
24 [“Land-Productivity Dynamics Towards Integrated Assessment of Land Degradation at  
25 Global Scales.” Technical Report EUR 26052. Joint Research Centre of the European  
26 Commission (2013)].

27 The LPD is the methodological basis of the R-based tool *LPDynR* presented in this  
28 document. It uses vegetation-related indices (phenology and productivity) derived from  
29 time series of remote sensed imagery to estimate ecosystem dynamics and change. The  
30 final result of the LPD indicator is a categorical map with 5 classes of land productivity  
31 dynamics, ranging from declining to increasing productivity. As an example of *LPDynR*  
32 functionalities, we present a case study for Europe.

## 33 **1 Introduction**

34 The United Nations General Assembly designed in 2015 a collection of 17 global goals,  
35 so called Sustainable Development Goals (SDGs; UN 2015), with the general aim of  
36 “achieving a better and more sustainable future for all”, and which were intended to be  
37 accomplished by the year 2030. Each SDG is subdivided into a list of targets which, in  
38 turn, go together with indicators to be able to measure their success. Such indicators have  
39 to be credible, based on standardized methodologies and, often, spatially explicit  
40 (Dubovský 2017).

41 The SDG-15, entitled Life on Land, has among its targets the 15.3, which expects “to  
42 combat desertification, restore degraded land and soil, including land affected by  
43 desertification, drought and floods, and strive to achieve a land degradation-neutral  
44 world”. In this context, Land Degradation Neutrality (LDN) is defined as the stable (or  
45 increasing) state regarding the amount and quality of land resources required to support  
46 ecosystem functions and services and enhance food security during a certain period of  
47 time (UNCCD 2015).

48 The indicator 15.3.1 is adopted to measure the LDN and is expressed as the proportion  
49 (%) of land that is degraded over total land area. It is a binary indicator (i.e. degraded/not  
50 degraded) based on three sub-indicators calculated separately: (1) Trends in Land Cover,  
51 (2) Land Productivity and (3) Carbon Stocks (Sims et al. 2017, 2020). While the first two  
52 can capture relatively fast changes, carbon stocks reflect slower changes which suggest a  
53 longer term trajectory (Orr et al. 2017). Following a “one-out-all-out” process, the  
54 indicator identifies an area as degraded if one of the sub-indicators shows degradation.

55 The three sub-indicators must be comparable among territories and based on standardized  
56 sources and methods. The data can be collected through existing sources, such as maps,  
57 reports or databases, but also can be derived from Earth Observation (EO) imagery using  
58 remote sensing tools.

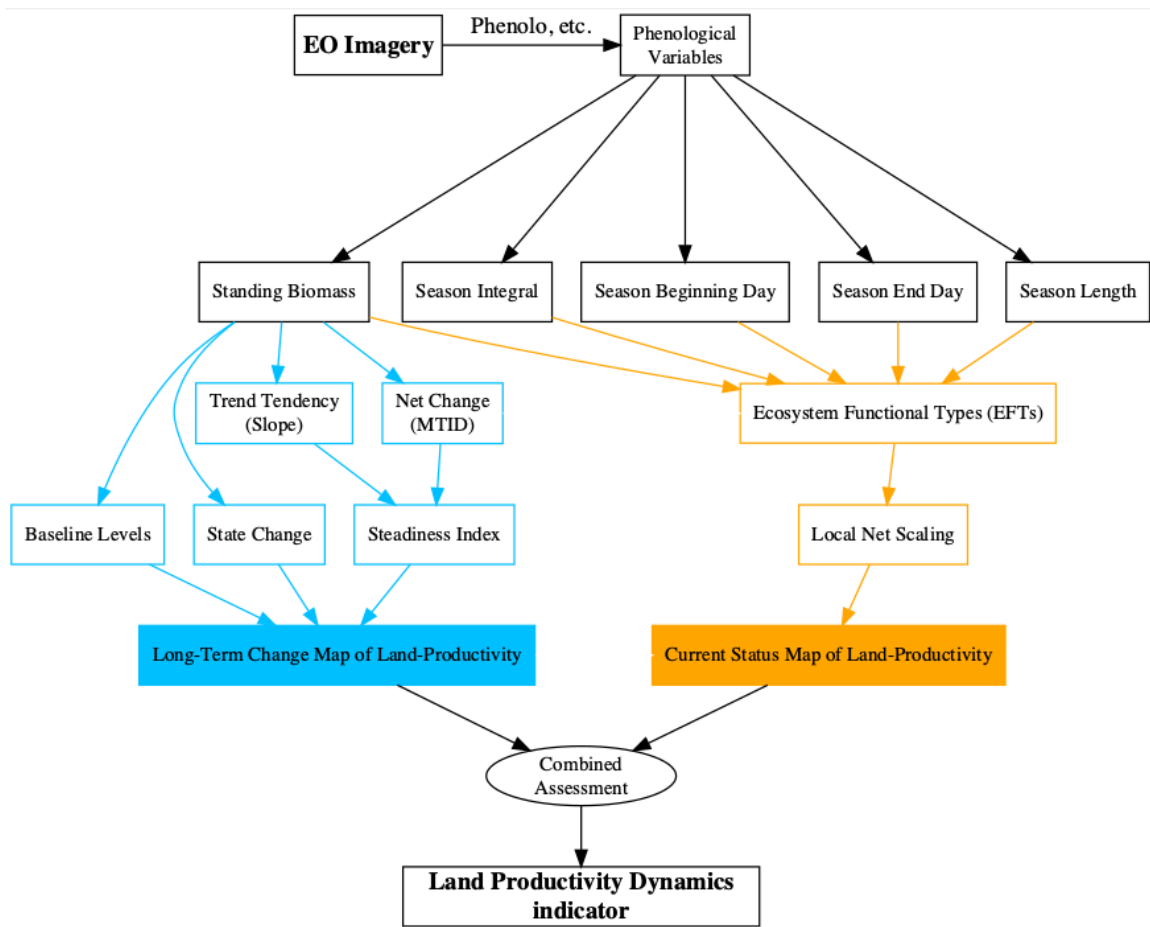
59 The Land Productivity sub-indicator (LP), addressed in this document, refers to the total  
60 above-ground net primary production (NPP), which can be defined as the total energy  
61 fixed by plants minus their respiration. Such energy is transformed into biomass which,  
62 in turn, allows ecosystems to develop their functions and deliver essential services.  
63 Therefore, LP reflects changes in health and productive capacity of the land and its

64 declining trends can be usually understood as land degradation (Cherlet et al. 2018;  
65 Prince 2009; Yengoh et al. 2015). The LP sub-indicator is calculated using the Land  
66 Productivity Dynamics (LPD) approach, first developed by Ivits and Cherlet (2013),  
67 which is the methodological basis of the *LPDynR* tool presented in this document.

## 68 **2 Land Productivity Dynamics and *LPDynR***

69 The Land Productivity Dynamics (LPD) approach is based fundamentally on the use of  
70 time series of vegetation-related indices derived from remote sensed imagery, such as the  
71 normalized difference vegetation index (NDVI) or the plant phenology index (PPI).  
72 NDVI, for example, can be used as a proxy for land productivity, as many studies at  
73 global and local scales have identified a strong relationship between NDVI and NPP  
74 (Ivits and Cherlet 2013; Prince 2009; Yengoh et al. 2015, and references therein). The  
75 LPD approach often uses phenological and productivity-related variables derived from  
76 time series of NDVI, given that these can provide additional information on several  
77 aspects of vegetation/land cover functional composition in relation to ecosystem  
78 dynamics and change (Ivits, Cherlet, Mehl, et al. 2013). These dynamics of the  
79 ecosystems, which eventually might drive to land degradation, can be caused by human  
80 activities and/or biophysical processes, as well as other processes not tied to them, such  
81 as climate change (Yengoh et al. 2015). While the most commonly used phenological  
82 parameters are the beginning and the end date of the vegetation growing season, together  
83 with the season length in number of days, the ones related to land productivity are those  
84 which approximates the measures to NPP and growing season production.

85 The final result of the LPD indicator is a categorical map with 5 classes of land  
86 productivity dynamics, ranging from declining to increasing productivity. It is the result  
87 of a combined assessment of two sources of information, as seen in Figure 1. On the one  
88 hand, the first layer is the Long Term Change Map. In general terms, it shows the  
89 tendency of change of land productivity (positive or negative) and the effect that this  
90 tendency might have had on a particular original point after a certain period of time. On  
91 the other hand, the second layer is the Current Status Map, which provides information  
92 on the current levels of land productivity in relation to its potential. It compares the local  
93 productivity with the range of productivity across similar areas in terms of land cover or  
94 bioclimatic traits (Sims et al. 2017). Further explanations for both branches will be given  
95 in their own sections below.



96

97 *Figure 1: Flowchart of the process to calculate the Land Productivity Dynamics indicator and*

98 *used by LPDynR*

99 Following the LPD approach, *LPDynR* is an R-based tool (i.e. an R package) which  
 100 allows the user to produce the final Land Productivity Dynamics Map using as inputs a  
 101 set of time series of phenological and/or productivity variables (multi-band GeoTIFF  
 102 rasters). By means of the different functions included in the package, it produces  
 103 intermediate layers (e.g. Steadiness Index, Ecosystem Functional Types, etc.) which are  
 104 used to calculate both the Long Term Change Map and the Current Status Map. In  
 105 addition, several parameters can be set along the process in order to fit them with the  
 106 preferences of the user. The functions included in the package have no limitations

107 regarding the number of years included in the time series, the variables to use or the  
108 spatial extent and resolution. The source code of the latest version of *LPDynR* can be  
109 found at <https://github.com/xavi-rp/LPDynR>.

110 **3 Data set preparation**

111 A case study is presented in this document in order to illustrate the methodology  
112 implemented in the *LPDynR* package to calculate the LPD indicator. In this case, it is  
113 used a data set of 3 phenological and productivity-related variables, at European level and  
114 0.5km of spatial resolution, produced and freely distributed by the European  
115 Environmental Agency - European Commission (<https://www.eea.europa.eu/data-and->  
116 maps/). They are all derived from time series (2000-2016) of MODIS imagery and its  
117 derived product Plant Phenology Index (PPI; Jin and Eklundh 2014). PPI is linearly  
118 related to the canopy green leaf area index (LAI) and has a temporal pattern very similar  
119 to the one shown by the gross primary productivity (GPP) estimated by flux towers at  
120 ground reference stations. The three variables are produced using the software TIMESAT  
121 (Jönsson and Eklundh 2004). More information about them can be found in their own  
122 webpage:

- 123 • Above ground vegetation productivity (from now on, CF):  
124 <https://www.eea.europa.eu/data-and-maps/data/annual-above-ground-vegetation->  
125 productivity
- 126 • Start of vegetation growing season (from now on, SBD): <https://www.eea.europa.eu/>  
127 [data-and-maps/data/annual-start-of-vegetation-growing\)](https://www.eea.europa.eu/data-and-maps/data/annual-start-of-vegetation-growing)

128 • Vegetation growing season length (from now on, SL):  
129 [https://www.eea.europa.eu/data-and-maps/data/annual-above-ground-vegetation-](https://www.eea.europa.eu/data-and-maps/data/annual-above-ground-vegetation-season)  
130 season)

131 In the *LPDynR* v.1.0.0, the functions use multi-band GeoTIFF rasters to start the process,  
132 one per phenological/productivity variable. Each band of each raster contains one of the  
133 years of the time series.

134 It is also important to notice that *LPDynR* comes with a small data set, which can be used  
135 to run tests, as well as some examples in the form of “vignettes” attached to the package.  
136 Once the package is installed, a basic example can be seen loading the following lines of  
137 R code:

```
138 # To install the latest version of LPDynR
139 library(devtools)
140 install_github("xavi-rp/LPDynR")
141
142 # Launching an example
143 library(LPDynR)
144 vignette(topic = "LPD_simple_example", package = "LPDynR")
```

145

## 146 4 Long Term Change Map of Land Productivity

147 As seen in Figure 1 and explained above, the Land Productivity Dynamics indicator is  
148 produced based in two different main layers, being the first one the Long Term Change  
149 Map (also called “tendency map”). In turn, this tendency incorporates information both  
150 on the progression of the general process of land dynamics (positive or negative) and on  
151 the original level of productivity of the ecosystem, as well as whether it has changed its  
152 state or not in the period under study (Ivits and Cherlet 2013). The multi-source

153 information used for the Long Term Change Map derivation is necessary because, for  
154 instance, even though an ecosystem presents a long term negative dynamics, it might  
155 have not been strong enough to decrease its level of productivity to change its original  
156 state. The way in which the three sources of information are calculated for the Long Term  
157 Change Map using a land productivity variable is described in the following subsections.

## 158 **4.1 Steadiness Index**

159 The first of the three metrics which integrates the Long Term Change Map represents the  
160 long term tendency of degradation of the natural systems on study, either positive or  
161 negative. This metrics is the “Steadiness Index” which, in turn, is based on the  
162 combination of two other metrics calculated per pixel: (1) the slope derived from a linear  
163 regression of the different years of the time series and (2) the net change of the  
164 productivity level on the same period.

165 The use of a linear regression would imply to respect some strict statistical assumptions  
166 for confidence intervals and significance tests to be representative. This is why the  
167 Steadiness Index only keeps classes of tendency and no more tests are run for assessing  
168 its significance. See Ivits and Cherlet (2013) for further explanations on this point.

169 Therefore, only the sign (positive or negative) of the slope of the trend is kept as the  
170 value of each pixel’s tendency of ecosystem dynamics. In addition, the net change of the  
171 productivity variable is calculated for the same time window and per pixel using the  
172 Multi-Temporal Image Differencing method (MTID; Guo et al. 2008). And, afterwards, it  
173 is transformed also into positive or negative net change. Finally, both metrics (slope of

174 the linear function and net change category) are combined to get four “steadiness”  
175 categories as seen in Table 1.

176 *Table 1: Description of the four Steadiness Index classes and how they are derived based on the*  
177 *combination of the signs of both the slope of the linear function and the net change*

Steadiness Class	Slope	Net Change	Description
Steadiness1	-	-	Strong negative ecosyst. dynamics (possibility changing equil.)
Steadiness2	-	+	Moderate negative ecosyst. dynamics (likely remain current equil.)
Steadiness3	+	-	Moderate positive ecosyst. dynamics (likely remain current equil.)
Steadiness4	+	+	Strong positive ecosyst. dynamics (possibility changing equil.)

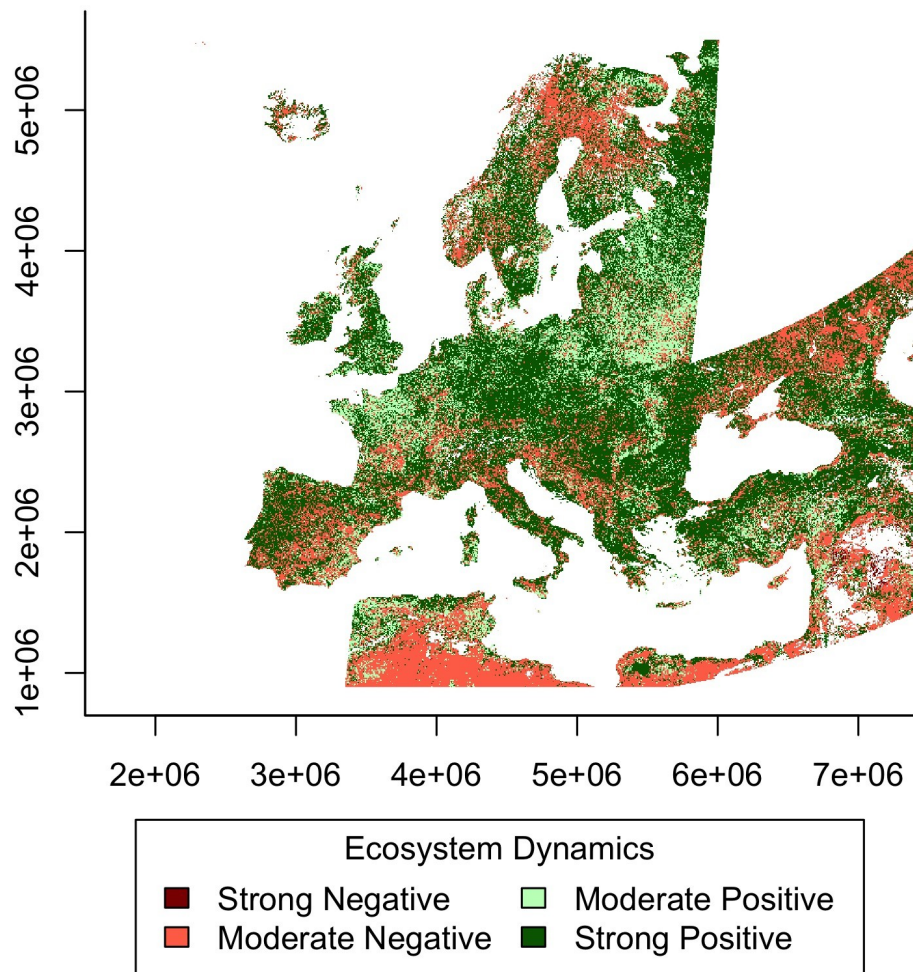
178

179 While Figure 2 represents a 4-class map of the Steadiness Index for the case study, the  
180 following lines of code show how to run the function *steadiness()* of the package to  
181 calculate the Steadiness Index.

```
182 ?steadiness
183
184 SteadInd <- steadiness(obj2process = cf, # 'cf' productivity
185 variable with time series
186 cores2use = 3,      # parallel processing
187 filename = "SteadInd.tif")
```

188

# Steadiness Index



189

190 *Figure 2: Representation of the Steadiness Index for the case study based on the 'Above ground*  
191 *vegetation productivity' variable*

## 192 **4.2 Baseline levels of the productivity variable**

193 The second source of information for the derivation of the Long Term Change Map is the  
194 baseline levels of the productivity variable in study, in the example case, the “Above  
195 ground vegetation productivity” variable.

196 For the calculation of the baseline levels of land productivity at the beginning of the time  
197 series on study, *LPDynR* categorizes the results into three classes: low, medium and high.  
198 To do that, the function *baseline\_lev()* averages the first *n* years of the time series in  
199 order to avoid extreme events such as abnormal droughts in wet areas, etc. This number  
200 of years can be set by passing the argument *yearsBaseline* to the function. Its default is 3,  
201 given that averaging more years would move the value closer to the mean of the time  
202 series, which is not desirable.

203 After the average is calculated, *baseline\_lev()* first classifies pixels into 10 classes instead  
204 of the final three (i.e. low, medium and high) using 10-quantiles. The reason for this  
205 intermediate step is that, if directly opted for three classes, the number of pixels per  
206 category would have been classified homogeneously (i.e. 33.3% of pixels/class), and this  
207 is in contrast with what is stated by the United Nations Development Programme (<https://www.undp.org>). UNPD declares that 40% of the World's land resources are drylands  
208 (Middleton et al. 2011) and, therefore, 40% of pixels at global level must be classified as  
209 "low level" of productivity. Consequently, as default, *LPDynR* classifies the first four  
210 groups of pixels as "low", whereas the five consecutive groups as "medium" and the rest  
211 10% of pixels with the largest baseline levels, as "high". Both the proportion of pixels  
212 classified as low level and high level of land productivity can be set by passing to  
213 *baseline\_lev()* the arguments *drylandProp* and *highprodProp*, respectively. The function  
214 classifies the rest of the pixels ((100 - (*drylandProp* + *highprodProp*)) as medium level.  
215 The assumption of classifying 40% of pixels as low productive is valid at global level,  
216 however, the proportion of drylands/low level of productivity should be modified for

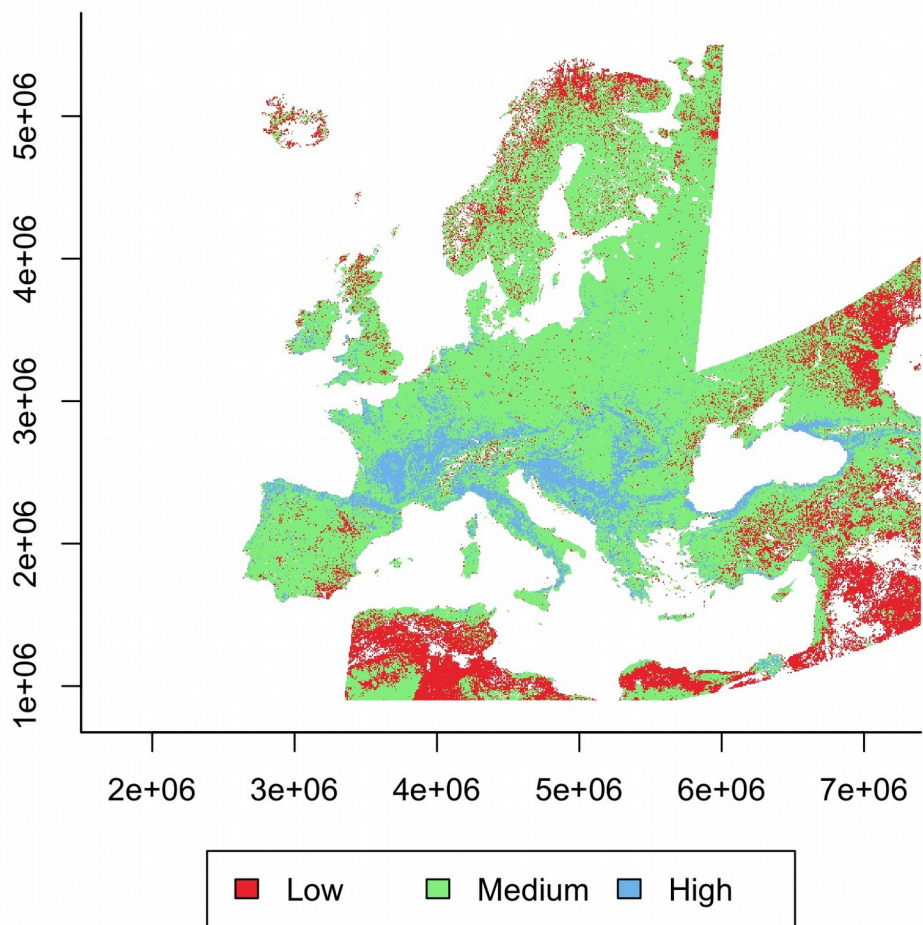
218 local and regional studies. For example, at the European level, drylands cover 20% of  
219 total land (FAO 2019).

220 In the following lines of code it can be observed how to run *baseline\_lev()* to categorize  
221 the baseline levels of productivity, while adjusting the parameters to the European  
222 proportion of drylands. The result is a final 3-class map showing the estimation of the  
223 levels of productivity at the beginning of the time series (Figure 3).

```
224 ?baseline_lev
225
226 Baseline_Level <- baseline_lev(obj2process = cf,
227                               yearsBaseline = 3,
228                               drylandProp = 0.2, # 20% dryland
229                               highprodProp = 0.1, # 10% highly
230                               productive land
231                               cores2use = 3,
232                               filename = "Baseline_Level.tif")
```

233

# Baseline Levels of Land Productivity



234

235 *Figure 3: Representation of the baseline levels of land productivity for the case study*

## 236 4.3 State Change of the productivity variable

237 The third layer used for the land productivity Long Term Change Map is the change of  
238 the state of the productivity variable during the time window of the study. This point is  
239 necessary for land degradation assessments as it reports whether productivity thresholds  
240 have been passed or not. The state change can be a consequence of either the natural

241 resilience thresholds have been surpassed or new land use/practices have been introduced  
242 by humans (Ivits and Cherlet 2013).

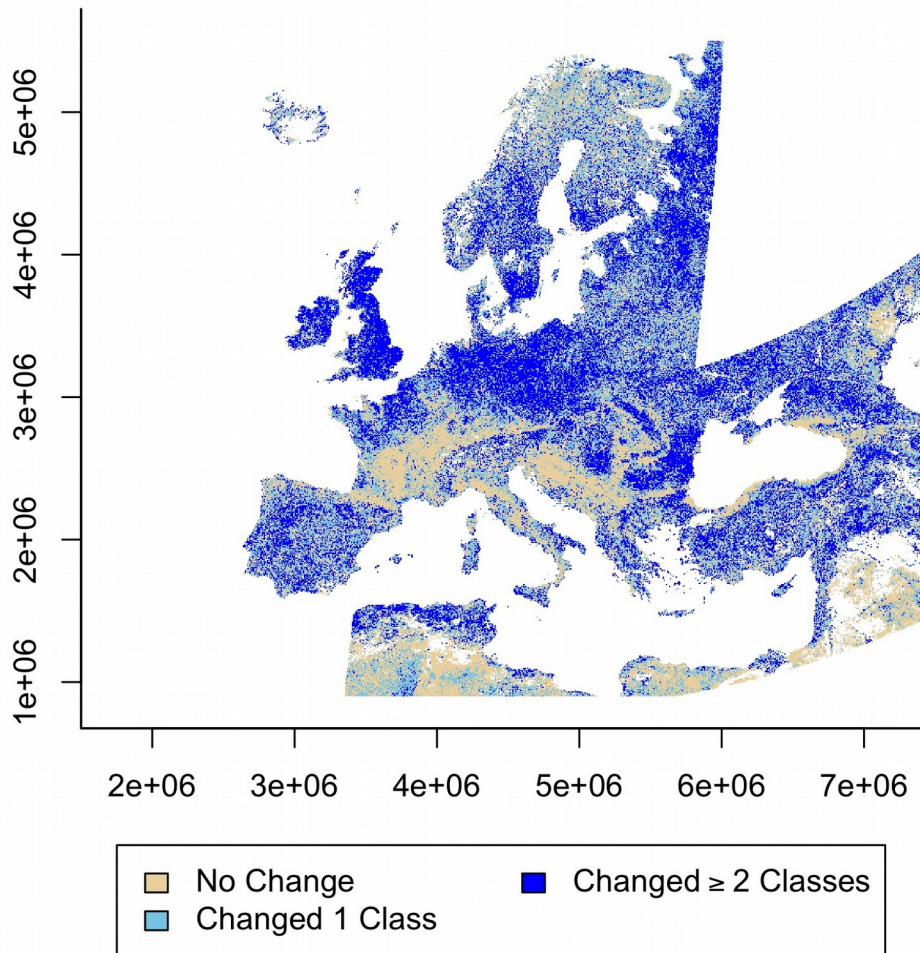
243 To calculate this state change per pixel, *LPDynR* uses both the state level at the beginning  
244 of the time series, as calculated in the previous subsection, and the state level at the end  
245 of the period. This final state is calculated in the same way than the base line level, i.e.  
246 (1) averaging the last 3 years and (2) classifying into 10 categories using 10-quantiles.  
247 The reason for not using the final 3-class classification is because it would be difficult to  
248 appreciate if the change of one state to another was due to a big or a small change.  
249 Instead, using the 10-class classification, one can see for instance if a pixel has moved  
250 from class 5 to 4 (small change) or from class 9 to 4 (big change).

251 Once the class change per pixel has been calculated, either with positive or negative  
252 results, the map is categorized into 3 final classes: (1) no change, (2) changed 1 class or  
253 (3) changed 2 or more classes. See Figure 4 for a map of the state change in the case  
254 study. The following code shows how to run the function *state\_change()* to perform the  
255 final classification.

```
256 ?state_change
257
258 State_Change <- state_change(obj2process = cf,
259                               yearsBaseline = 3,
260                               cores2use = 3,
261                               filename = "State_Change.tif")
```

262

# Change of Land Productivity Classes



263

264 *Figure 4: Representation of the state change map of the productivity variable (baseline levels  
265 minus final levels), after being reclassified into 3 categories (1: no change; 2: changed 1 class;  
266 3: changed 2 or more classes) for the case study*

## 267 4.4 Land Productivity Long Term Change Map

268 The land productivity Long Term Change Map is one of the two pillars of the LPD  
269 indicator (Figure 1) calculated with *LPDynR*. This map is developed, in turn, by the  
270 combination of the Steadiness Index, the productivity levels at the beginning of the time

271 series and the change of the state of productivity between the beginning and the end of  
272 the time series, all calculated with the productivity variable in use.

273 The function *LongTermChange()* (see an example of running it below) performs the  
274 combination of the three qualitative metrics mentioned before into the Long Term  
275 Change Map, resulting in 22 new categories as shown in Table 2. The resulting map for  
276 the case study is presented in Figure 5.

```
277 ?LongTermChange  
278  
279 Long_Term_Change_Map <- LongTermChange(SteadinessIndex = SteadInd,  
280  
281 BaselineLevels =  
282 Baseline_Level,  
283 StateChange = State_Change,  
284  
285 filename =  
286 "Long_Term_Change_Map.tif")
```

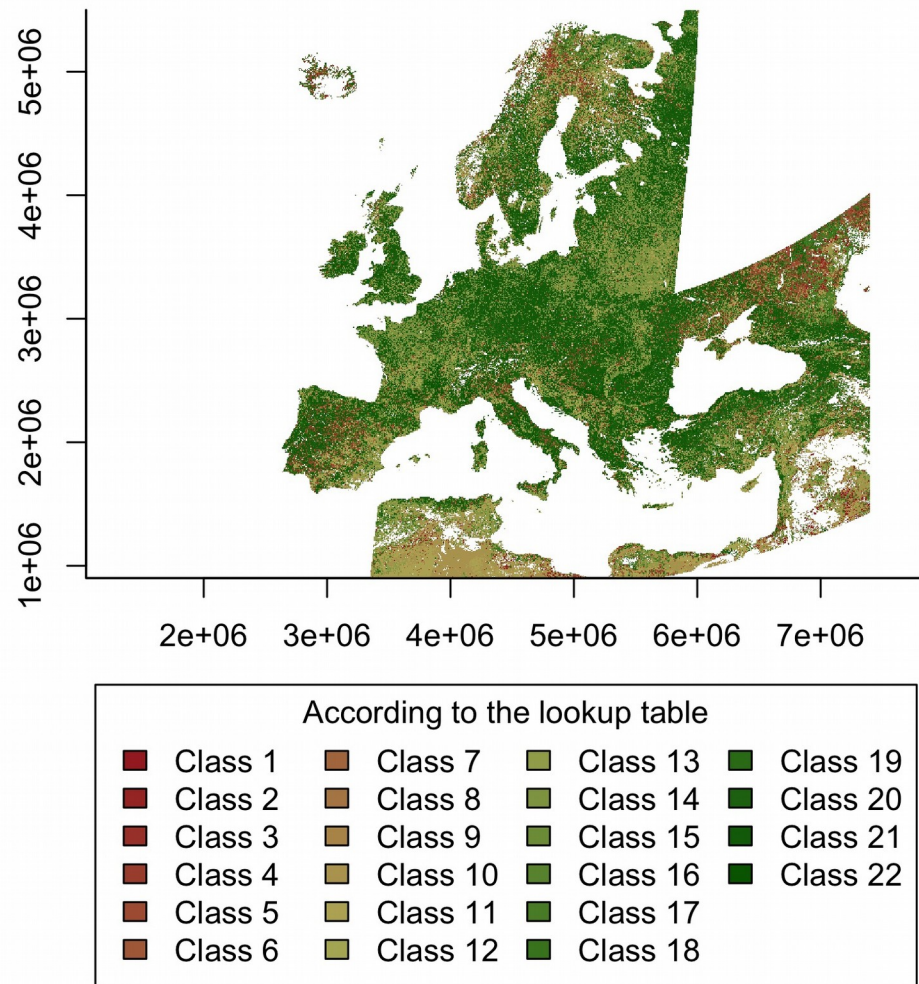
287

288 *Table 2: Lookup table for the land productivity Long Term Change Map (Steadiness Index +*  
289 *BaseLine Levels + State Change)*

Class Change Stead.Ind. / BaseL.	No Change	Changed 1 class	Changed ≥ 2 classes
<b>St1 low</b>	1	2	3
<b>St1 med.</b>	4	5	6
<b>St1 high</b>	7	8	9
<b>St2 low</b>	10	10	10
<b>St2 med.</b>	11	11	11
<b>St2 high</b>	12	12	12
<b>St3 low</b>	13	13	13
<b>St3 med.</b>	14	14	14
<b>St3 high</b>	15	15	15
<b>St4 low</b>	16	17	18
<b>St4 med.</b>	19	20	21
<b>St4 high</b>	22	22	22

290

## Long Term Change Map



291

292 *Figure 5: Land productivity Long Term Change Map for the case study based on the combination*  
293 *of the Steadiness Index, the baseline levels and change of states of land productivity*

294

295 At this point, the user might want to finalise the LPD calculation avoiding the second part  
296 of the methodology proposed by Ivits and Cherlet (2013), which is the Current Status

297 Map of Land Productivity. In this case, the function *LPD\_CombAssess* (see further  
298 explanations in its own subsection below) can be called to reclassify the 22-class Long  
299 Term Change Map into the final 5 classes of LPD. In the following code it can be seen an  
300 example of how to run the function to perform the reclassification.

```
301 ?LPD_CombAssess  
302  
303 LPD_finalMap <- LPD_CombAssess(LandProd_change =  
304 Long_Term_Change_Map,  
305                                     LandProd_current = NULL,  
306                                     filename = "LPD_finalMap.tif")  
307  
308 plot(LPD_finalMap)  
309
```

## 310 **5 Current Status Map of Land Productivity**

311 The Land Productivity Dynamics indicator is composed by two base layers, as shown in  
312 Figure 1. After the long term productivity dynamics described previously (i.e. Long Term  
313 Change Map), the second source of information needed is the current level of land  
314 productivity. For this purpose, a Local Net Scaling approach is implemented (Prince  
315 2009). Such approach estimates, by means of Earth Observation imagery and remote  
316 sensing tools, the level of land productivity of each pixel relative to its neighbours with  
317 similar characteristics. In other words, it calculates the potential level of productivity of  
318 each pixel within a homogeneous land unit at the time under study. The Current Status  
319 Map may help, for instance, to identify areas which, although having a positive trend of  
320 productivity over time, their levels of current productivity are low relative to the pixels in  
321 the same homogeneous land unit and, thus, they might be still suffering land degradation

322 (Sims et al. 2017). A first step for the calculation of the Current Status Map, therefore,  
323 must be the derivation of the homogeneous land units across the area of study.

324 **5.1 Ecosystem Functional Types (EFTs)**

325 The methodology implemented in *LPDynR* to derive homogeneous land units, or  
326 Ecosystem Functional Types (EFTs), is adapted from Ivits, Cherlet, Horion et al. (2013).  
327 It is basically a clustering process which uses, in this case, phenological and productivity  
328 variables to create the groups. Among the different unsupervised clustering techniques  
329 available for data grouping, K-means has been chosen. K-means is widely used in data  
330 science mainly due to its relative simplicity.

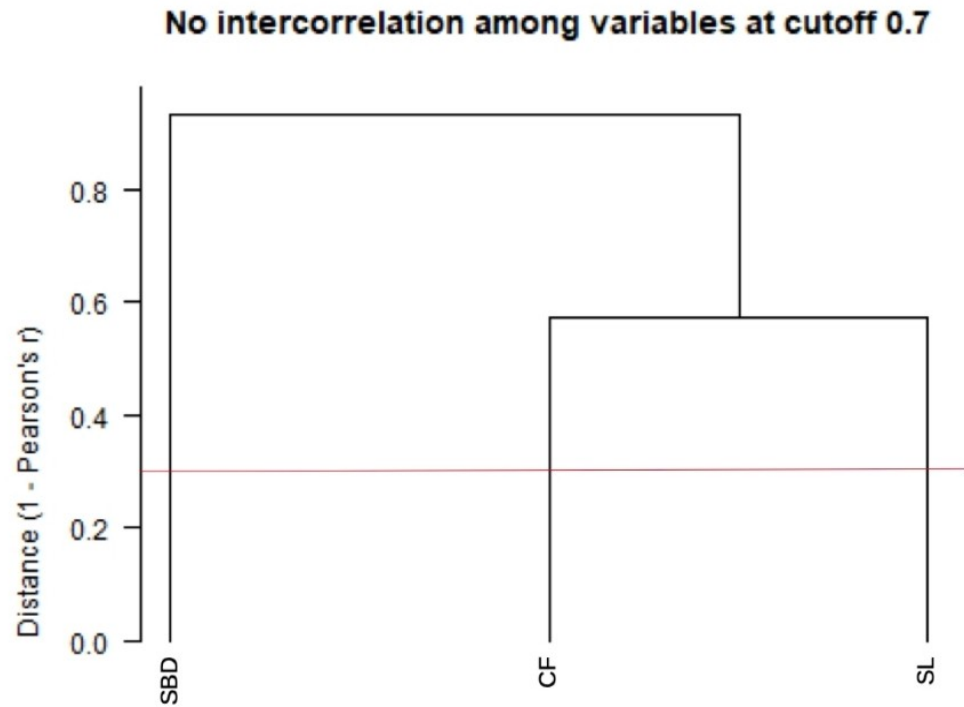
331 Originally, the unsupervised classification was performed after a three-steps  
332 preprocessing of the variables: (1) removing highly correlated variables; (2) a first  
333 Principal Component Analysis to know the optimal number of PCs and their associated  
334 variables showing the highest loadings; and (3) a final PCA to clearly associate each PC  
335 with one variable. However, some recent tests have shown that the final LPD indicator  
336 does not differ significantly when it is derived using the raw phenological/productivity  
337 variables. Therefore, although the two-PCAs step is also implemented in *LPDynR*, only  
338 removing those highly correlated variables (e.g.  $|r| > 0.7$ ) is recommended before to run  
339 the k-means clustering.

340 In order to check for multicollinearity among the variables, the function *rm\_multicoll()*  
341 first calculates their averages among the years of the time series. Then, the process  
342 internally runs the function *removeCollinearity()* from the package *virtualspecies*. This  
343 function allows the user to set up the minimum Pearson's correlation absolute value,

344 which is established to be 0.7 as default. It is also allowed to use a subset of random  
345 points of the data set to calculate the correlation in case the rasters have a large number of  
346 pixels and the user wants to speed up the process. The default number of randomly  
347 selected points is 10% of total pixels in the raster. Finally, one of the variables of each  
348 group of correlation is randomly selected. A dendrogram to visualize the groups of  
349 intercorrelated variables can be plotted. Figure 6 shows a dendrogram for the present case  
350 study, which has been run with three variables and no intercorrelation has been found  
351 among them at the cutoff 0.7. In the following piece of code it can be seen an example of  
352 how to run *rm\_multicol()* with all the mentioned parameters.

```
353 ?rm_multicol
354
355 variables_noCor <- rm_multicol(dir2process = variables_dir,
356                                     multicoll_cutoff = 0.7,
357                                     cores2use = 3,
358                                     filename = "variables_noCor.tif",
359                                     # The following arguments are
360                                     passed to virtualspecies:removeCollinearity()
361                                     sample.points <- TRUE # using
362                                     'nb.points' (or 10% of pixels) to calculate multicollinearity
363                                     nb.points <- 1000000
364                                     plot <- FALSE # if TRUE it writes
365                                     out a dendrogram
366                                     )
```

367



368

369 *Figure 6: Dendrogram of groups of correlated variables (none in this case). Multicollinearity*  
 370 *cutoff set to  $r > |0.7|$ . SBD: Start of vegetation growing season; SL: Vegetation growing season*  
 371 *length; CF: Above ground vegetation productivity*

372

373 In case the user would like to run the two-PCAs step, both the first “screening PCA”,  
 374 which is done over the uncorrelated variables, and the “final PCA” are subsequently  
 375 performed with the same function *PCAs4clust()*. In order to know the optimal number of  
 376 variables to be used in the “final PCA”, a threshold of cumulative variance of the PCs is

377 implemented. This threshold is established to be 0.9 as default. The following code shows  
378 an example of how to run this process.

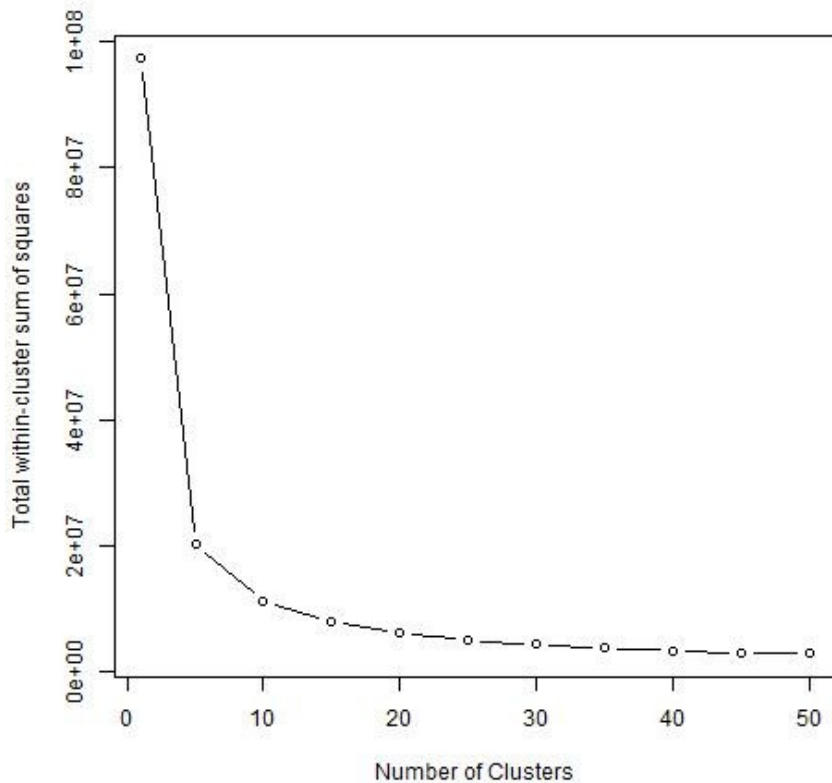
```
379 ?PCAs4clust
380
381 pca_final_brick <- PCAs4clust(obj2process = variables_noCor,
382                               cumul_var_threshold = 0.9,
383                               filename = "pca_final_brick.tif")
```

384

385 Finally, the clustering algorithm can be run over either the selected PCs or the  
386 uncorrelated raw variables using the function *EFT\_clust()*. This function uses *kmeans()*  
387 from the package *stats*. K-means is an iterative unsupervised method which has as one of  
388 the main limitations the fact that it is not able to optimize the number of clusters by itself.  
389 Instead, the optimal number of clusters needs to be calculated externally. In this case, it  
390 can be determined using the “scree-plot method”. Such method is implemented in  
391 *LPDynR* with the function *clust\_optim()* and it is based on running several K-means  
392 clustering with different number of clusters each, in order to assess how the quality of the  
393 models change with the number of clusters. Then, a plot is produced with the results and  
394 an “elbow” indicates where the quality of the model no longer improves substantially as  
395 the number of clusters (model complexity) increases. See Figure 7 for the results of the  
396 example presented in this document and the following code as an example of how to call  
397 the function. Notice that the clustering has been run with nine different number of  
398 clusters to give a good amount of points to plot the curve. And also that the maximum  
399 number of iterations is set up to 10. Although it is unlikely that the process gets any  
400 convergence with such a low number of iterations, the results are already valid for the  
401 purpose.

```
402 ?clust_optim  
403  
404 jpeg("OptimalNumClusters.jpg")  
405 clust_optim(obj2clust = pca_final_brick,  
406             num_clstrs = seq(5, 50, 5)  
407             )  
408 dev.off()
```

409



410

411 *Figure 7: "Scree plot" method used to calculate the optimal number of clusters. The "elbow"*  
412 *indicates where the quality of the model no longer improves substantially as the number of*  
413 *clusters (model complexity) increases*

414

415 The “scree plot” method undoubtedly has some level of subjectivity, as the user decides  
416 where the curve flattens enough. Alternatively, to remove such subjectivity, several  
417 numerical methods exist to calculate the optimal number of clusters, although they take  
418 also some statistical assumptions. These methods could be explored in the future if a  
419 higher level of accuracy is believed as necessary or if the whole process wants to be done  
420 without user’s intervention. In addition, other hierarchical clustering methods could be  
421 explored in order to avoid calculating the optimal number of clusters beforehand,  
422 although previous tests run with ISODATA have been shown to be highly resource  
423 demanding, especially in terms of computing time.

424 Once the optimal number of clusters is estimated, the final clustering is run with the  
425 function *EFT\_clust()*. It is important to notice that when setting *nstart*, the larger, the  
426 more accurate result. This is because the function uses different sets of starting random  
427 centroids and runs the clustering *nstart* times, and the best result is chosen. Therefore, a  
428 larger *nstart* increases the chances of having a better cluster classification. *EFT\_clust()*  
429 provides, together with a RasterLayer object with the clusters, a clustering performance  
430 evaluator. This value is calculated by the ratio of *betweenss* (i.e. between-cluster sum of  
431 squares) and *totss* (i.e. total sum of squares), in percentage, and it is expected to be as  
432 high as possible.

433 In addition, *k-means()* can use different algorithms to perform the clustering (e.g.  
434 “MacQueen”, “Hartigan-Wong”, etc.). As stated in the function documentation (*?k-*  
435 *means*), “Hartigan-Wong” usually gives better results, although it is recommended to try  
436 several starts (*nstart > 1*). However, when using “Hartigan-Wong” with a (too) large  
437 number of clusters, and a lot of values of the variables are very similar, *k-means()* is not

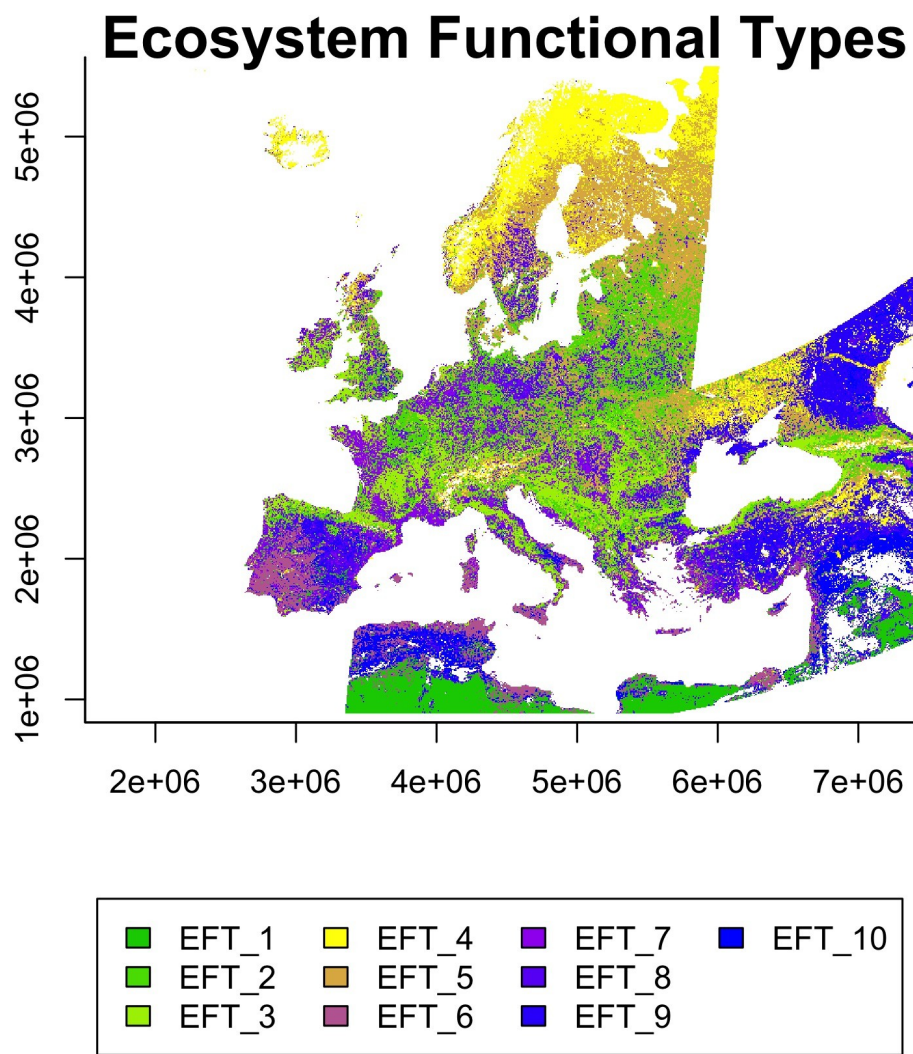
438 able to converge in an acceptable amount of time (even increasing the number of  
439 iterations). In these cases, the user has to be careful because *k-means()* only gives a  
440 warning, so the final clustering is based on a non converged process. Diminishing the  
441 number of clusters or rounding variables' values might be good strategies to help *k-*  
442 *means()* to converge.

443 Finally, as previous tests of K-means with up to 100 iterations were not converging, the  
444 maximum number of iterations is set to 500 as default. Within this limit and rounding  
445 variables, for almost all the tests performed, the process did achieve convergence.

446 For the running example, the EFTs resulted from the whole process can be seen in Figure  
447 8. In addition, the following code shows an example of the function call using the  
448 *BrickLayer* object produced in the previous step with *rm\_multicol()*, and setting the  
449 optimal number of clusters estimated with *clust\_optim()*, together with a *nstart* value  
450 higher than 1 and the algorithm to be used.

```
451 ?EFT_clust
452
453 EFTs <- EFT_clust(obj2clust = variables_noCor,
454                      n_clust = 20,
455                      nstart = 5,
456                      algorithm = "Hartigan-Wong",
457                      filename = "EFTs.tif")
458
459 clust_eval <- EFTs[[2]]      # Evaluation of clustering performance
460 EFTs <- EFTs[[1]]          # RasterLayer object with the clusters
```

461



462

463 *Figure 8: Ecosystem Functional Types (EFTs) derived from phenological and productivity*  
 464 *variables using the K-means clustering method for the case study*

465

## 466 5.2 Local Net Production Scaling

467 The Local Net Primary Production Scaling (from now on, Local Net Scaling or LNS)  
 468 method (Prince 2009) is based on the use of multi-temporal satellite data to calculate the

469 difference between the potential and actual NPP for each pixel in homogeneous land  
470 areas. It will be considered potential productivity to that productivity which would have  
471 been without the influence of human factors, and it is estimated as the maximum value of  
472 productivity within each EFT (Prince 2009, and references therein). The current land  
473 production related to the local potential reflects the current level of productivity  
474 efficiency and, therefore, it is useful for the delineation of a productivity status map (Ivits  
475 and Cherlet 2013).

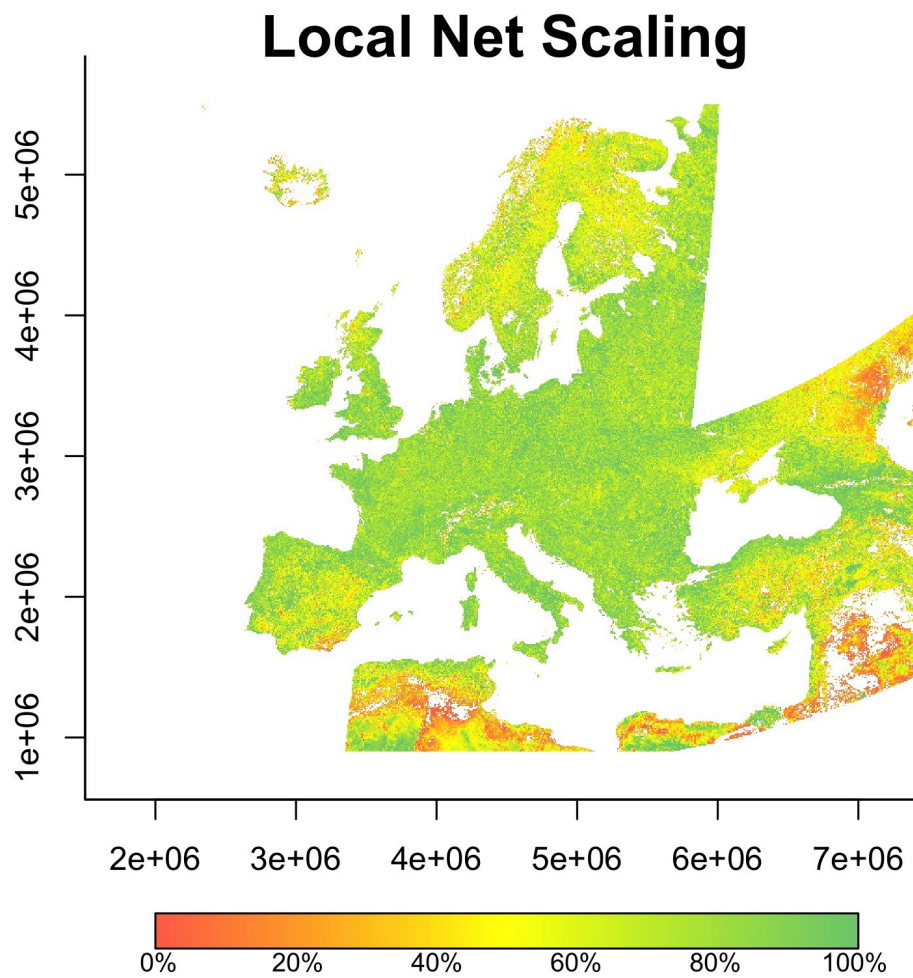
476 The cyclic fraction of vegetation productivity, or the summed NDVI over the growing  
477 season, is widely used as a proxy for the estimation of the current land productivity  
478 (Fensholt 2013), as it incorporates both natural and anthropogenic factors which define  
479 the inter-annual variability of land production. Therefore, it represents that part of the  
480 standing biomass which is potentially appropriated to be used by humans and the  
481 environment (Ivits and Cherlet 2013).

482 The function *LNScaling()* is implemented in *LPDynR* to calculate the LNS. In the case  
483 study, the above ground vegetation productivity variable (i.e. CF) for the period between  
484 2000 and 2016 has been passed to the function, which runs the LNS using the average of  
485 the last 5 years. Together with the productivity variable, the EFTs calculated previously  
486 are also passed to the function, and the potential productivity within each EFT is  
487 calculated. However, instead of the maximum value within each cluster, its 90-percentile  
488 is established as the final potential, given that values higher than this threshold can be  
489 considered as outliers. Finally, the LNS per pixel is calculated as the proportion of its  
490 annual production (i.e. the average of 5 years cyclic fraction) over the potential  
491 production within its EFT (i.e. the 90-percentile). The result for the case study is

492 represented in Figure 9, and the following lines of code show an example on how to call  
493 the function.

```
494 ?LNScaling  
495  
496 LNScal <- LNScaling(EFTs = EFTs, # RasterLayer with the EFTs  
497 ProdVar = cf, # Productivity variable  
498 cores2use = 3,  
499 filename = "LNScal.tif")
```

500



501

502 *Figure 9: Local Net Primary Production Scaling (LNS): proportion of annual production (i.e.*  
503 *average of the last 5 years of cyclic fraction) over the local potential production (i.e. the 90-*  
504 *percentile within the Ecosystem Functional Type)*

505

506 For the calculation of the final LPD indicator (i.e. Combined Assessment), these levels of  
507 local productivity will be aggregated into two categories: (1) pixels with less than 50% of  
508 the highest annual local production (within the EFT) and (2) pixels with more or equal to  
509 50% of annual local production.

## 510 **6 Combined Assessment of Land Productivity**

511 The Land Productivity Dynamics indicator, as shown in the flowchart of the process for  
512 its derivation in Figure 1, is based on the combination of two main sources of  
513 information: a map of the tendency, positive or negative, of the level of land productivity  
514 along the time series, and another map capturing the current level of productivity of each  
515 pixel relative to the maximum productivity in a homogeneous land area. As seen above in  
516 this document, both branches to calculate the indicator are qualitative methods.

517 Therefore, the final LPD indicator is also a qualitative measure with 5 possible values or  
518 categories after the reclassification of each pixel as shown in Table 3. Such categories are  
519 (1) d - Declining, (2) ew - Early signs of decline, (3) nf - Stable but stressed, (4) pf -  
520 Stable and not stressed and (5) i - Increasing land productivity.

521 *Table 3: Lookup table for the combination of the two branches assessment (i.e. Long Term*  
 522 *Change Map and Current Status Map of land productivity) to derive the Land Productivity*  
 523 *Dynamics categories (i.e. (1) d - Declining land-productivity, (2) ew - Early signs of decline of*  
 524 *land productivity, (3) nf - Stable but stressed land productivity, (4) pf - Stable and not stressed*  
 525 *land productivity and (5) i - Increasing land productivity)*

Steadiness I.	Baseline L.	State Change	Local Sc.	
			< 50%	>= 50%
st1	lo	0	d	ew
st1	lo	1	d	ew
st1	lo	2	d	d
st1	me	0	d	ew
st1	me	1	d	ew
st1	me	2	d	d
st1	hi	0	ew	nf
st1	hi	1	d	ew
st1	hi	2	d	ew
st2	lo	0	nf	nf
st2	me	0	nf	nf
st2	hi	0	nf	nf
st3	lo	0	pf	pf
st3	me	0	pf	pf
st3	hi	0	pf	pf
st4	lo	0	pf	i
st4	lo	1	pf	i
st4	lo	2	i	i
st4	me	0	pf	i
st4	me	1	i	i
st4	me	2	i	i
st4	hi	0	i	i

526

527 In the case study presented in this document, the Land Productivity Dynamics indicator  
 528 final map (Figure 10) is the result of the combined assessment of the Long Term Change

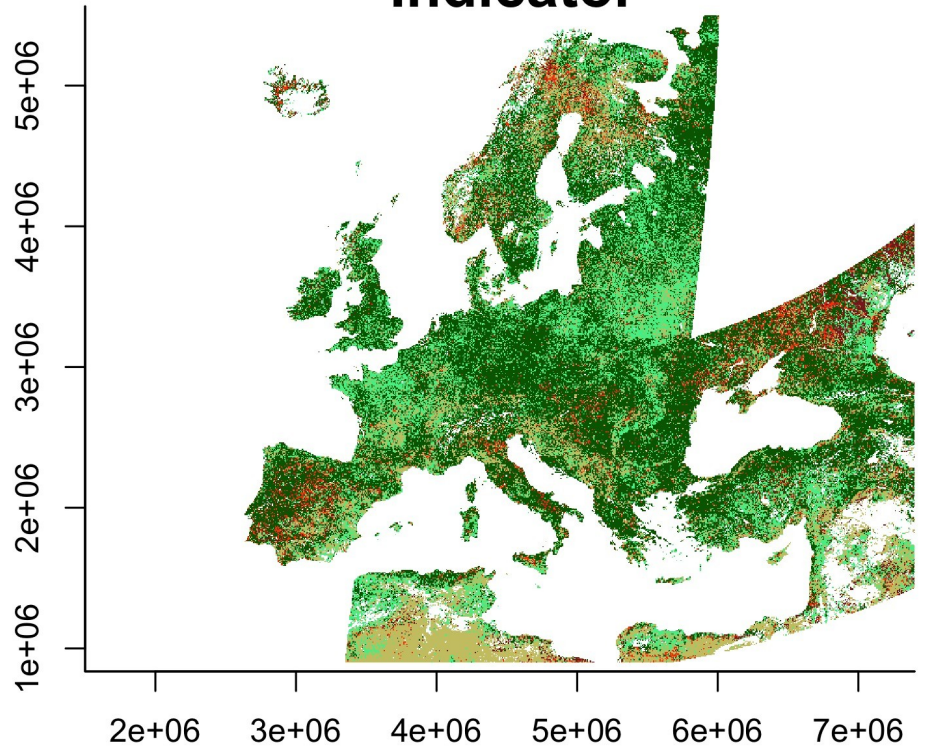
529 Map (Figure 5) and the Current Status Map of land productivity (Figure 9), both based on  
530 the “above ground vegetation productivity” variable.

531 The function to run the combined assessment to calculate the LPD indicator is  
532 *LPD\_CombAssess()* and the following code shows an example of how to call it.

```
533 ?LPD_CombAssess  
534  
535 LPD_finalMap <- LPD_CombAssess(LandProd_change =  
536 "Long_Term_Change_Map",  
537 LandProd_current = "LNScal",  
538 filename = "LPD_finalMap.tif")  
539  
540 plot(LPD_finalMap)
```

541

## Land Productivity Dynamics Indicator



- 1(d): Declining land productivity
- 2(ew): Early signs of decline of land productivity
- 3(nf): Negative fluctuation (stable, but stressed land prod.)
- 4(pf): Positive fluctuation (stable, not stressed land prod.)
- 5(i): Increasing land productivity

542

543 *Figure 10: Land Productivity Dynamics indicator final map. Combined assessment of the Long  
544 Term Change Map and the Current Status Map of land productivity.(1) d - Declining land-  
545 productivity, (2) ew - Early signs of decline of land productivity, (3) nf - Stable but stressed land  
546 productivity, (4) pf - Stable and not stressed land productivity and (5) i - Increasing land  
547 productivity*

548

549 **6.1 Alternative method for the LPD indicator**

550 It has been shown previously that it is important to include in the LPD calculation the  
551 current level of land productivity relative to its potential, given that it may indicate  
552 degradation in areas with a positive tendency of productivity, but where the level of  
553 productivity still remains low relative to other similar areas nearby. Despite this, the user  
554 might want to derive the final product based only on the tendency map (i.e. Long Term  
555 Change Map), avoiding the inclusion of the Current Status Map derived with the Local  
556 Net Scaling approach. The function *LPD\_CombAssess()* has the potentiality to do it by  
557 passing the argument *LandProd\_current = NULL*. By doing so, the function reclassifies  
558 the Long Term Change Map into the same 5 categories of the LPD indicator described  
559 above, as shown in Table 4.

560 *Table 4: Lookup table for the reclassification of the Long Term Change Map into the Land  
561 Productivity Dynamics categories (i.e. (1) d - Declining land-productivity, (2) ew - Early signs of  
562 decline of land productivity, (3) nf - Stable but stressed land productivity, (4) pf - Stable and not  
563 stressed land productivity and (5) i - Increasing land productivity)*

Steadiness I.	Baseline L.	State Change	LPD class
st1	lo	0	<b>d</b>
st1	lo	1	<b>d</b>
st1	lo	2	<b>d</b>
st1	me	0	<b>d</b>
st1	me	1	<b>d</b>
st1	me	2	<b>d</b>
st1	hi	0	<b>ew</b>
st1	hi	1	<b>d</b>
st1	hi	2	<b>d</b>
st2	lo	0	<b>nf</b>
st2	me	0	<b>nf</b>

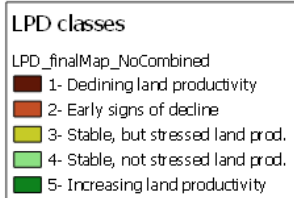
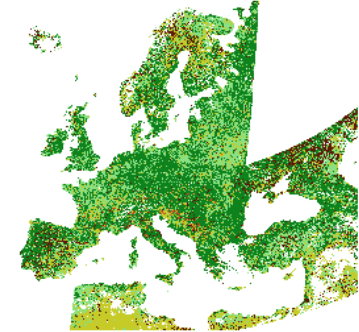
st2	hi	0	<b>nf</b>
st3	lo	0	<b>pf</b>
st3	me	0	<b>pf</b>
st3	hi	0	<b>pf</b>
st4	lo	0	<b>pf</b>
st4	lo	1	<b>pf</b>
st4	lo	2	<b>i</b>
st4	me	0	<b>pf</b>
st4	me	1	<b>i</b>
st4	me	2	<b>i</b>
st4	hi	0	<b>i</b>

564

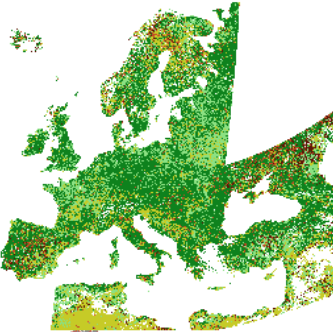
565 A comparison of the final LPD indicator map produced using the Combined Assessment  
 566 (i.e. Long Term Change Map + Current Status Map) with the one developed avoiding the  
 567 Current Status Map for the case study can be seen in Figure 11 (Map 1 and Map 2,  
 568 respectively). In addition, the “differences map” in the same figure represents those  
 569 pixels showing a different class from one approach to the other. Notice that this  
 570 difference is always equal to minus 1, which means that the pixels only change 1 class  
 571 and that the Combined Assessment has always classes with larger values (i.e. better  
 572 conditions in terms of land productivity). Table 5 shows the number of pixels which  
 573 change from one class to another. From this table it can be seen how pixels never change  
 574 from negative to positive dynamics (class 3 to 4) or from positive to negative (class 4 to  
 575 3).

## Comparison LPD final maps produced with Combined Assessment and with reclassification of Long Term Change Map

Map 1: LPD final map (Reclass of tendency map)



Map 2: LPD final map (Combined Assessment)



576

577 *Figure 11: Land Productivity Dynamics indicator final maps derived by the reclassification of*  
578 *the Long Term Change Map of land productivity (Map 1) and produced by the Combined*  
579 *Assessment (Map 2; Long Term Change Map + Current Status Map). Differences Map (Map 1 -*  
580 *Map2) represents in red those pixels showing different resulting classes from both approaches.*

581

582

583

584

585 *Table 5: Number of pixels showing different class in the Combined Assessment approach and in*  
586 *the non combined one (i.e. reclassification of the Long Term Change Map). Only these three*  
587 *combinations have been found in the case study*

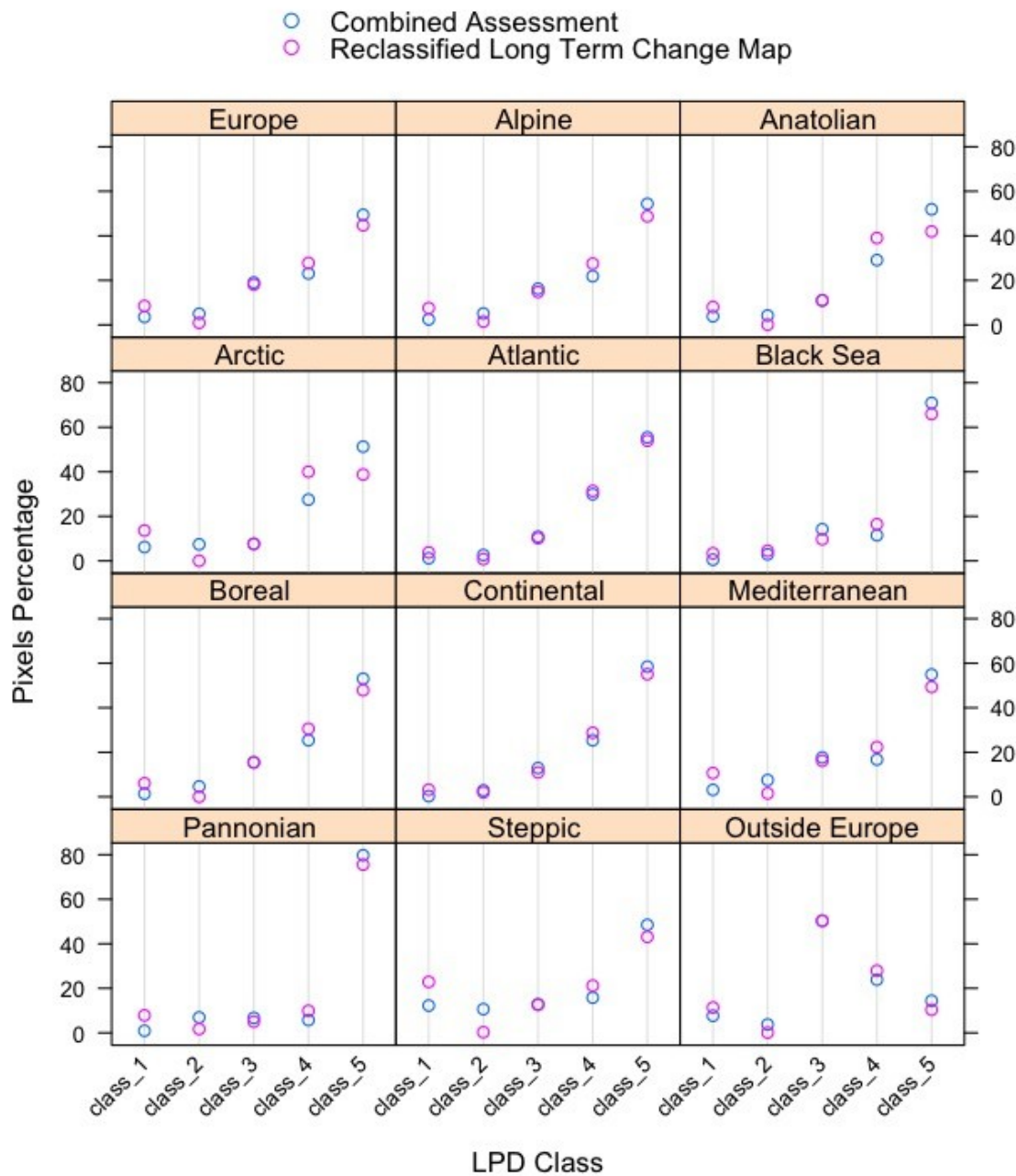
No Combined Assessment - Class	Combined Assessment - Class	Number Pixels	Description
1	2	1861147	Declining to Early signs of decline
2	3	334957	Early signs of decline to Stable but stressed
4	5	1772401	Stable not stressed to Increasing

588

589 Finally, Figure 12 shows the proportion of pixels per LPD class under each approach,  
590 both for the whole extent (i.e. Europe) and also splitting the map by biogeographical  
591 regions. The biogeographical regions have been defined with the official delineations  
592 used in the Habitats Directive (92/43/EEC) and for the EMERALD Network, which are  
593 freely distributed as a spatial data set by the European Environmental Agency - European  
594 Commission ([https://www.eea.europa.eu/data-and-maps/figures/biogeographical-and-](https://www.eea.europa.eu/data-and-maps/figures/biogeographical-and-marine-regions-in)  
595 marine-regions-in).

596 The plots show that there are some differences in the proportion of pixels per class for  
597 each of the two approaches. For example, the Anatolian, the Arctic and the Steppic  
598 regions are the three showing more differences, which range from 10 to 12.5% for some  
599 LPD classes. This fact supports the importance of including the Current Status Map in the  
600 calculations to refine the LPD indicator final results.

## Comparison LPD Methods by Bio-Geographical Regions (Combined Assessment vs LongTermChangeM Reclassification)



601

602 *Figure 12: Proportion of pixels per LPD class for the Combined Assessment (light blue) and for*  
 603 *the reclassified Long Term Change Map (purple), for Europe and by biogeographical regions*

604

605 **6.2 Land Productivity Dynamics partial indicator**

606 As seen in the previous subsections regarding the derivation of the tendency map (i.e.  
607 Long Term Change Map), its final result is quite related to the extremes of the time  
608 series. Then, if the time series is long, the LPD indicator shows a big picture of what has  
609 happened regarding the land productivity dynamics between the beginning and the end of  
610 the period under study. However, to understand the dynamics of the biomass within this  
611 period of time, as well as to assess the stability of the final product, it might be useful to  
612 produce several “partial LPD indicators” using different time windows of the time series.

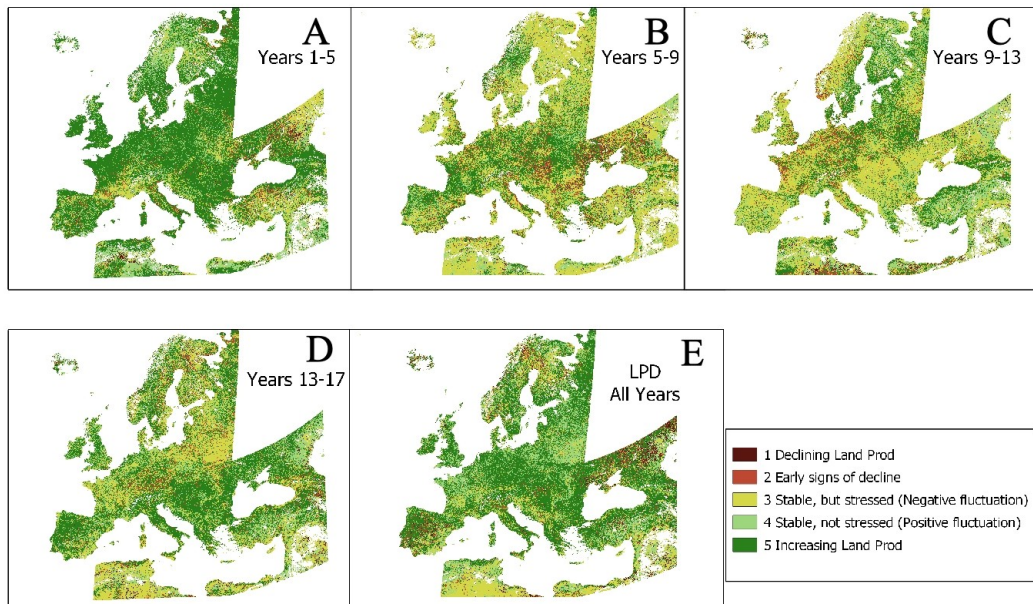
613 This process is not yet implemented in *LPDynR* but we propose the following code to  
614 produce partial LPD maps of  $n$  years and with an overlap of  $y$  years between the end of  
615 the last period and the beginning of the next one. This example is implemented for the  
616 same case study shown along this document and the final partial LPD maps can be seen  
617 in Figure 13.

618

```
619 ## Running LPDynR for partial time series ##
620
621 ts_length <- 5                                # time series length
622 to run 'partial LPD maps'
623 ts_years_overlap <- 1                          # number of years of
624 overlapping
625 partial_dir <- "/LPD_partial"                 # directory to save
626 the 'partial LPD' results
627 first_year <- 1                               # first year of the
628 whole time series
629 last_year <- nlayers(cf)                      # last year of the
630 whole time series
631 last_year_run <- first_year + ts_length - 1  # last year of the
632 'partial LPD'
633
634 while(last_year_run <= last_year){
635   # subsetting the years (layers) to run
636   cf_run <- cf[[first_year:last_year_run]]
```

656

## Partial LPD Indicators



657

658 *Figure 13: Partial LPD indicators (plots A to D) and LPD indicator for the whole time series*  
659 *(plot E). The partial LPD indicators have been produced for time windows of 5 years with an*  
660 *overlap of 1 year between the end of the last period and the beginning of the next one*

661

662 The complete LPD indicator (i.e. for the whole time series; Figure 13E) shows, in general  
663 terms, a positive trend pattern across Europe (i.e. more pixels in greens). However, the  
664 intermediate plots, especially Figure 13B to D, show more negative trends (i.e. yellow  
665 and light red pixels). In addition, the first partial indicator shows much more increasing  
666 land productivity in the period between years 1 to 5. This, besides demonstrating the  
667 highly fluctuating character of vegetation, confirms the influence of the extremes of the  
668 time series on the final result. In this sense, in the time series of the example, the first  
669 year(s) seems to be quite low in terms of productivity for most of the pixels in  
670 Central/Northern Europe, and they suffer a big increase around years 5/6. Such increase  
671 causes a large number of areas belonging to the higher LPD class, and it still influences  
672 the dynamics of the following periods, resulting in areas with stressed vegetation.

673 The fact that the LPD indicator calculated with the approach included in *LPDynR* is quite  
674 influenced by the beginning and the end of the time series does not suppose a limitation,  
675 but it is convenient as the main goal of the LPD indicator is to know the current state of  
676 vegetation in relation to a distant previous state, and not the fluctuations due, for  
677 example, to exceptional or unusual climatic events.

678 **7 Conclusions**

679 As stated by the Intergovernmental Science-Policy Platform on Biodiversity and  
680 Ecosystem Services (IPBES), land degradation leads to a loss of biodiversity and a  
681 reduction of ecosystem functions and delivered services all over the world. Therefore,  
682 combating land degradation and restoring degraded lands has become an urgent priority  
683 in order to protect all life on Earth as well as to ensure human well-being (IPBES 2018).  
684 In this sense, satellite observations provide valuable data which might help to monitor the  
685 Earth's land cover to evaluate the state of land degradation.  
  
686 The Land Productivity Dynamics indicator (LPD), as part of the SDG-15.3.1 indicator,  
687 aims at assessing the state of land degradation and desertification at global, regional and  
688 local scales. In turn, the *LPDynR* tool presented in this document has been developed to  
689 derive the LPD indicator using phenological and land productivity variables, which have  
690 been obtained from long-term time series of earth observation imagery.  
  
691 *LPDynR* is a comprehensive set of programming code, written in the well-known R  
692 language and properly packaged, ready to be freely distributed in order to let the users  
693 with a minimum knowledge of the R language calculate the LPD indicator. The package,  
694 once installed, includes several examples and a small data set for testing the  
695 functionalities and the different parameters to tune them. The open source code of  
696 *LPDynR* version 1.0.0 can be found and installed from  
697 <https://github.com/xavi-rp/LPDynR>.

698 **8 References**

- 699 Cherlet, M., C. Hutchinson, J. Reynolds, J. Hill, S. Sommer, and G. von Maltitz, eds.
- 700 2018. *World Atlas of Desertification*. Luxembourg: Publication Office of the
- 701 European Union.
- 702 Dubovyk, Olena. 2017. “The Role of Remote Sensing in Land Degradation Assessments:
- 703 Opportunities and Challenges.” *European Journal of Remote Sensing* 50 (1): 601–
- 704 13. <https://doi.org/10.1080/22797254.2017.1378926>.
- 705 FAO. 2019. “Trees, Forests and Land Use in Drylands: The First Global Assessment.”
- 706 FAO Forestry Paper 184. Rome: FAO.
- 707 Fensholt, Kjeld Kaspersen, Rasmus Rasmussen. 2013. “Assessing Land
- 708 Degradation/Recovery in the African Sahel from Long-Term Earth Observation
- 709 Based Primary Productivity and Precipitation Relationships.” *REMOTE SENSING*
- 710 5 (2): 664–86.
- 711 Guo, W. Q., T. B. Yang, J. G. Dai, L. Shi, and Z. Y. Lu. 2008. “Vegetation Cover
- 712 Changes and Their Relationship to Climate Variation in the Source Region of the
- 713 Yellow River, China, 1990–2000.” *International Journal of Remote Sensing* 29 (7):
- 714 2085–2103. <https://doi.org/10.1080/01431160701395229>.
- 715 IPBES. 2018. “The Ipbes Assessment Report on Land Degradation and Restoration.
- 716 Montanarella, L., Scholes, R., and Brainich, a. (Eds.).” Bonn, Germany: Secretariat
- 717 of the Intergovernmental Science-Policy Platform on Biodiversity; Ecosystem
- 718 Services.

- 719 Ivits, E., and M. Cherlet. 2013. "Land-Productivity Dynamics Towards Integrated  
720 Assessment of Land Degradation at Global Scales." Technical Report EUR 26052.  
721 Joint Research Centre of the European Commission.
- 722 Ivits, E., M. Cherlet, S. Horion, and R. Fensholt. 2013. "Global Biogeographical Pattern  
723 of Ecosystem Functional Types Derived from Earth Observation Data." *Remote  
724 Sensing* 5 (7): 3305–30. <https://doi.org/10.3390/rs5073305>.
- 725 Ivits, E., M. Cherlet, W. Mehl, and S. Sommer. 2013. "Ecosystem Functional Units  
726 Characterized by Satellite Observed Phenology and Productivity Gradients: A Case  
727 Study for Europe." *Ecological Indicators* 27: 17–28.  
728 <https://doi.org/10.1016/j.ecolind.2012.11.010>.
- 729 Jin, Hongxiao, and Lars Eklundh. 2014. "A Physically Based Vegetation Index for  
730 Improved Monitoring of Plant Phenology." *Remote Sensing of Environment* 152:  
731 512–25. <https://doi.org/https://doi.org/10.1016/j.rse.2014.07.010>.
- 732 Jönsson, P., and L Eklundh. 2004. "TIMESAT—a Program for Analyzing Time-Series of  
733 Satellite Sensor Data." *Computers & Geosciences* 30: 833–45.
- 734 Middleton, N., L. Stringer, A. Goudie, and D. Thomas. 2011. "The Forgotten Billion.  
735 MDG Achievement in the Drylands." New York, NY, 10017, USA: United Nations  
736 Development Programme.
- 737 Orr, B. J., A. L. Cowie, V. M. Castillo Sanchez, P. Chasek, N. D. Crossman, A. Erlewein,  
738 G. Louwagie, et al. 2017. "Scientific Conceptual Framework for Land Degradation  
739 Neutrality. In: A Report of the Science-Policy Interface." Bonn, Germany:  
740 UNCCD.

- 741 Prince, I. Rishmawi, S. D. Becker-Reshef. 2009. "Detection and Mapping of Long-Term  
742 Land Degradation Using Local Net Production Scaling: Application to Zimbabwe."  
743 *REMOTE SENSING OF ENVIRONMENT* 113 (5): 1046–57.
- 744 Sims, N. C., C. Green, G. J. Newham, J. R. England, A. Held, M. A. Wulder, and et al.  
745 2017. *Good Practice Guidance Sdg Indicator 15.3.1. Proportion of Land That Is  
746 Degraded over Total Land Area*. First. United Nations Convention to Combat  
747 Desertification.
- 748 Sims, Neil C., Nichole N. Barger, Graciela I. Metternicht, and Jacqueline R. England.  
749 2020. "A Land Degradation Interpretation Matrix for Reporting on Un Sdg  
750 Indicator 15.3.1 and Land Degradation Neutrality." *Environmental Science &  
751 Policy* 114: 1–6. <https://doi.org/https://doi.org/10.1016/j.envsci.2020.07.015>.
- 752 UN. 2015. "Transforming Our World: The 2030 Agenda for Sustainable Development."  
753 A/RES/70/1. United Nations.
- 754 UNCCD. 2015. "Integration of the Sustainable Development Goals and Targets into the  
755 Implementation of the United Nations Convention to Combat Desertification and  
756 the Report of the Intergovernmental Working Group on Land Degradation  
757 Neutrality." ICCD/COP(12)/4. Ankara, Turkey: UNCCD Conference of the Parties.
- 758 Yengoh, G. T., D. Dent, L. Olsson, A. E. Tengberg, and C. J. Tucker. 2015. *Use of the  
759 Normalized Difference Vegetation Index (Ndvi) to Assess Land Degradation at  
760 Multiple Scales*. Springer Briefs in Environmental Science. Springer.